Jurnal Kejuruteraan 36(5) 2024: 2179–2189
https://doi.org/10.17576/jkukm-2024-36(5)-35

Effects of Spans and Heights of Half-Cuboctahedron Tensegrity Roof Subjected to Wind Loading

Nabihah Jamal[a], Oh Chai Lian[b*], Mohd Raizamzamani Md Zain[b], Lee Siong Wee[c] & Norrul Azmi Yahya[c]

[a] *IJM Construction Sdn Bhd, 19th Floor, Unit 19-03, City Plaza, Jalan Tebrau, 80250 Johor Bahru, Malaysia*

[b]*School of Civil Engineering, Universiti Teknologi MARA, Shah Alam 40450, Selangor, Malaysia*

[c]*School of Civil Engineering, College of Engineering, Universiti Teknologi MARA, 81750, Masai, Johor, Malaysia*

**Corresponding author: chailian@uitm.edu.my*

Received 29 February 2024, Received in revised form 11 June 2024
Accepted 11 July 2024, Available online 30 September 2024

ABSTRACT

Tensegrity structures are a type of structural system that consists of a specific set of cables connected to a rigid body configuration and stabilised by internal cable forces in the absence of external forces. Since tensegrity structures appear in lightweight features, wind-induced vibrations in roof structures increase the importance of structural design. Thus, this study analysed the effect of heights and spans towards half-cuboctahedron tensegrity roof model subjected to wind loading. The proposed grid's heights are 0.5m, 1,0m and 1,5m. To conduct this study, the basic component of half-cuboctahedron consists of 12 cables and 4 struts were modelled first by using SAP2000 software. The basic model has been extended into another 4 units for the short span (2x2) model and another 16 units (4x4) for a long span model. The design parameters such as material and section properties, supports and loads subjected to the structure have been proposed as the provision laid down in Eurocode Standard. This study found that the deflection decreased apparently from a height of 0.5 m to 1.0 m up to about 40%. Analysis reveals that the span length is a more critical factor in determining deflection compared to the model's height. An analysis of varying strut diameters was conducted to assess their impact on the demand capacity ratio. The findings demonstrated a decrease in diameter led to a higher demand capacity ratio. From the evaluation, struts with diameter 48.3 mm is the optimum size to be used for tensegrity roof model. The study provides understanding of the behaviour of tensegrity roof grid model subjected to wind loading.

Keywords: Demand-Capacity Ratio, Half-Cuboctahedron, SAP2000, Tensegrity, Wind.

INTRODUCTION

The term tensegrity is coined by the words ‘‘tension’’ and ‘‘integrity’’. It is an inventive concept in the field of structural engineering. A tensegrity structure typically comprises a set of discontinuous compression members connected by a set of continuous tensile members. Tensile forces in tensegrity structures are controlled by their inner self-stress state, unlike conventional cable structures. As a result, tensegrity structures are self-supporting and do not require costly anchorages. Applications of tensegrities in architecture, engineering structures, robots and biology were explored (Panigrahi et al., 2009; Oh et al. 2012; Oh et al. 2022; Gómez-Jauregui et al. 2023).

There is substantial literature on the mathematical formulation in form-finding the tensegrity models (He et al. 2024; Oh et al. 2020). However, studies on the design of the large roof tensegrity structures remain open (Hanaor & Liao, 1991). Most investigations on tensegrity still focus on the theoretical and performance aspects rather than design and construction (Panigrahi et al. 2009). Only a few presented fabrication, instrumentation, and non-destructive testing on tensegrity structures. Non-destructive static and dynamic testing on a bio-based tensegrity

prototype for measuring prestress of the system consisting bamboo culms for the struts and sisal ropes for the cable nets (de Albuquerque et al. 2022). The experimental studies reported in the literature are restricted to small models only. A study compared the behaviour of steel half-cuboctahedron and hexagonal tensegrity grid roof models under various load combinations (Panigrahi et al. 2009). The study found that the half-cuboctahedron grid roof is a more feasible configuration for large-span roof structures from the standpoint of strength and serviceability compared to the hexagonal tensegrity grid roof. The finding is supported by a detailed investigation from Parthasarathi et al. (2016), who found a half-cuboctahedron roof grid more practicable for a large-span roof structure than the hexagonal grid tensegrity systems. The study investigated mechanisms of half-cuboctahedron tensegrity roof models under wind load. A study of different grid sizes of the half-cuboctahedron grid tensegrity systems in roof structures also reveals the potential application for larger span structures (Sulaiman et al. 2016).

The conception and design of self-stressed, spatial, and reticulate tensegrity roofs are complex, involving large computational time (Quirant et al. 2003). As a result, the studies on the complete design of the tensegrity structures as alternate roofs for modern structural systems are limited and not practically utilised. Since structural instability is a dynamic process by nature, understanding the mechanical behaviour of tensegrity structure is vital to aid in preventing the structure from sudden collapse, mainly for the lightweight features, when subjected to various loadings like winds, earthquakes, traffic, and waves (Martínez et al. 2019). Therefore, this study aims to investigate the effects of spans and height on the behaviour of tensegrity roof grids under wind loads. The study also evaluated load carrying capacity based on various strut diameter.

This paper presents the numerical analysis of half-cuboctahedron roof models using SAP2000. The remainder of the paper is organised as follows: Section 2 presents the methodologies on the analysis and design of the basic half-cuboctahedron grid model with different heights (i.e. 0.5 m, 1.0 m and 1.5 m) using SAP2000, which the grid model is then extended to 2×2 m grid and 4×4 m grid. Section 4 discusses the analysis results based on the struts' nodal deflections, axial forces, and demand capacity ratio. Lastly, the conclusions are drawn in Section 5.

METHODOLOGY

SELECTION OF GRID MODEL

Figure 1 depicts the three-dimensional view of the basic half-cuboctahedron module, which serves as a reference to construct larger models of roof grids 2 × 2 m and 4 × 4 m that represent the arrangement of four basic modules and sixteen basic modules, respectively. The basic half-cuboctahedron module consists of four cables that connect the lower (as well as the upper) end of struts to form lower (as well as the upper) square surfaces. The remaining four cables connect the lower and upper ends of the cables vertically. Geometrical data of the basic half-cuboctahedron module is presented in the Appendix. Table A1 lists the nodal coordinates for the basic half-cuboctahedron with different heights (0.5 m, 1.0 m and 1.5 m), whereas Table A2 lists the element connectivity for cables (elements 1-13) and struts (elements 14-17). The definition of the elemental connectivity of a basic module is essential to establish larger tensegrity systems combining many basic modules. SAP2000's replicate option was used to generate the 2 × 2 m and 4 × 4 m tensegrity roof grid model from the basic half-cuboctahedron module.

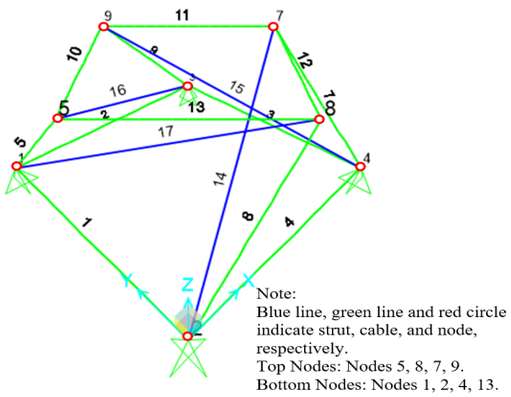

FIGURE 1. 3-Dimensional view of basic half-cuboctahedron tensegrity model

INITIAL PRE-STRESSING FORCES

Knowing that tensegrity is a pre-stressed system, initial pre-stressing forces need to be determined for the models before any application of forces. Pre-stress is important to keep the tensegrity maintain its shape and integrity. Alterations of prestress levels can change the stiffness and form of the tensegrity. By setting the input of pre-stressing forces SAP2000 auto-calculated the geometry and sag of the cables in the analysis and design processes. The undeformed relative length should be less than or equal to 1.0 to ensure that the cables are taut.

Considering the equilibrium of forces at all nodes, the pre-stressing forces (i.e. initial axial force) can be calculated using the form-finding method presented by Oh et al. (2020). Equilibrium equation for the whole tensegrity model is expressed as:

$$F = Bn \tag{1}$$

where B is a matrix consisting of directional cosines, F is a vector of nodal forces, and n is a vector of axial forces.

Moore-Penrose generalised inverse is used to obtain a solution of a rank-deficient system of equilibrium equations. The solution for the axial force vector $\boldsymbol{n}$ for the tensegrity module is given for the case of self-equilibrated state without external forces (such as F =0) by making use of Moore-Penrose generalised inverse:

$$n = [I_m - B^{+}B]\beta \tag{2}$$

where I is a vector of arbitrary coefficient of size m which m is numbers of element.

Applying eigenvector basis decomposition method, and assuming that the model has q number of independent self-equilibrium stress modes, Equation (2) can be further rewritten as

$$\ddot{\mathbf{0}} = \sum_{i=1}^{q} \beta_i^{*} \quad {}_i \tag{3}$$

Φ is an orthogonal matrix whose i^{th} column Φ_i (i = 1, 2, ... , m) corresponds to eigenvector associated with eigenvalue.

In an iterative process, a combination of β_i is used to determine the possible axial force $\boldsymbol{n}$ that satisfies the following inequality constraints derived from the elastic condition of the material properties as follows:

$$\begin{aligned} 0 \le n_c &\le \sigma_c A_c \\ -\frac{\pi^2 E_s I_s}{{l_s}^2} &\le n_s \le \sigma_s A_s \end{aligned} \tag{4}$$

where n_c, σ_c and A_c are axial forces, yield stress and cross-sectional area for cable elements, respectively; n_s, E_s, I_s, L_s, σ_s and A_s are axial forces, Young modulus, moment inertia of section, element current length, yield stress and cross-sectional area for strut elements, respectively.

Table 1 shows the initial pre-stress forces for the cables and struts in the basic half-cuboctahedron tensegrity model. The value of -9000 was used to obtain the initial pre-stress forces, which sufficiently make the cable stressed before assigning any load on the model.

TABLE 1. Initial pre-stressing forces

Element Number	Initial Pre-stressing Force (kN)	Description
1,2,3,4	1.357	Bottom cables
5,7,8,9	1.919	Leg cables
10,11,12,13	1.919	Top cables
14,15,16,17	-3.324	Struts

MATERIAL AND SECTION PROPERTIES

Since the sectional properties can significantly affect the structural behaviour, different strut diameters were investigated to evaluate the effectiveness of the tensegrity roof grid model subjected to wind loading. In the first phase, as the basis of the study, struts are assigned with Grade 355 circular steel hollow sections with an outer diameter of 76.1 mm, while cables have a diameter of 28.6 mm.

In the second phase, design optimisation via evaluation of the demand capacity ratio was conducted for another two different strut diameters. Demand capacity ratio reveals the maximum loads that a structure can safely withstand. Table 2 shows the sectional and material properties of struts and cables.

BOUNDARY CONDITIONS

This section describes the boundary conditions imposed on the tensegrity roof grid model, such as the supports and loadings. It is to be noted that there is no moment and rotational displacements in the pinned jointed tensegrity model. Pinned supports were assigned at the base of the half-cuboctactahedron module, at nodes 1, 2, 3 and 4 (refer Figure 1). When the module extended to 2×2 m and 4×4 m grid models, the pinned supports were assigned at the four corners and mid-point of the base.

Since tensegrity structures are in a self-equilibrium state, the self-weight can be neglected (Branam et al. 2019). This study considers a steel sheet flat galvanised with a 1 mm thickness, giving a total dead load of 0.3 kN/m^2. The live load of 0.4 kN/m^2 was used for the roof, which was not intended for accessibility except for regular maintenance and repair (category H). These values are chosen according to the provisions in EN 1991- 1-1. The basic wind speed of 33.5 m/s was considered for the target area in Shah Alam. The proposed building height for this study is 15 m. The design wind pressures for windward and leeward direction were computed as 0.348 kN/m^2 and -0.348 kN/m^2, respectively, in accordance with Section 2 of MS 1553.

Based on the limit state principle, different load combinations were considered in this study to determine which load combination is more critical for the structure.

A limit state can be defined as a structural state that represents the acceptable limit of some aspect of structural behaviour. Ultimate Limit State (ULS) is concerned with the structure's strength and stability under the maximum design load that the structure is expected to bear. Serviceability Limit State (SLS) refers to the condition beyond which specified service requirements, such as excessive deflection and cracking, are no longer met. In this study, the load combinations for each limit state were applied as shown in Table 3.

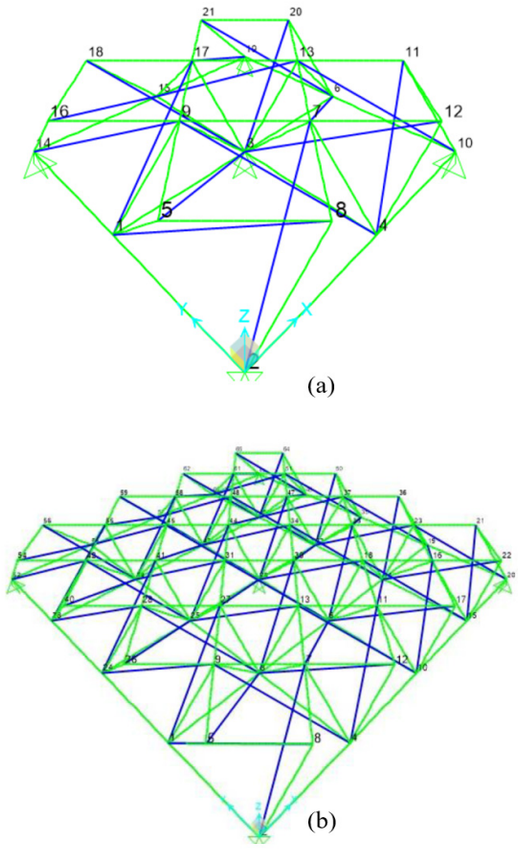

FIGURE 2. Half-cuboctahedron tensegrity grid roof model (a) 2 × 2 m grid and (b) 4 × 4 m grid

TABLE 3. ULS and SLS load combinations

Cases	DL	LL	WL
ULS 1	1.35	1.5	-
ULS 2	1.35	1.5	0.75 (WW)
ULS 3	1.35	1.5	0.75 (LW)
SLS 4	1.0	1.0	-

Note: ULS, SLS, DL, LL, WL, WW, LW denote Ultimate Limit State, Serviceability Limit State, dead load, live load, wind
load, windward, leeward, respectively.

The methodology can be summarized in the flow chart as shown in Figure 3.

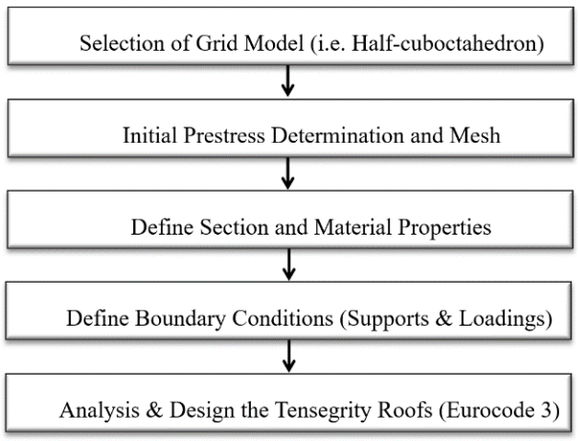

FIGURE 3. General Methodology Flow Chart

TABLE 2. Section and material properties

Member	Type	Diameter mm	Wall thickness mm	Young Modulus MPa	Area mm^2	Moment of Inertia mm^4	Poisson's ratio	Yield stress MPa	Unit weight kN/m^3
Strut (Analysis 1)	Circular hollow section	76.1	3.2	2.1×10^5	732.90	487800	0.3	355	78.5
Strut (Analysis 2)	Circular hollow section	21.3	2.3	2.1×10^5	137.28	6285	0.3	355	78.5
Strut (Analysis 3)	Circular hollow section	48.3	3.0	2.1×10^5	426.94	109995	0.3	355	78.5
Cable	Cable	28.6	-	1.9×10^5	645.16	33122	0.3	355	78.5

RESULTS AND DISCUSSION

EFFECTS OF HEIGHT AND SPAN IN DEFLECTIONS OF TENSEGRITY ROOF

The half-cuboctahedron tensegrity grid models of sizes 2×2 m and 4×4 m with different heights (0.5 m, 1.0 m and 1.5 m) were analysed using SAP2000. Structural behaviours such as deflections and axial forces were discussed in this section.

Figures 4(a) and 4(b) show the nodal displacements observed in 2×2 m and 4×4 m grid models, respectively. The trends observed in both the 2×2 m and 4×4 m grid models were expected: as the height of the model increased, the deflection decreased, particularly from 0.5 m to 1.0 m. This study found that deflection decreased by approximately 40% when the height increased from 0.5 m to 1.0 m. This finding is consistent with the results of a previous study by Panigrahi et al. (2009). However, there are no significant effects on the deflection for the height of the model at 1.0 m and 1.5 m. This is due to the adequacy of the structural height in sustaining the applied loadings and provision for the deflection control at 1.0 m. For the 2×2 m grid model, the highest deflection occurred at nodes 5, 12, 18 and 20, located the furthest away from the support and directly subjected with loadings (see Figure 5). A similar trend is also observed in the 4×4 m grid model analysis results.

Table 4 shows maximum deflections for the analysis models. The deflections were reduced up to 38% and 39% when the model's height of 0.5 m increased to 1.0 m for both 2×2 m and 4×4 m grid models, respectively. The changes in height from 1.0 m to 1.5 m show a deflection reduction of only about 1% to 2%. In addition, when comparing the nodal deflection at various spans, the 4×4 m grid model exhibits a higher deflection (more than 300%) than the 2×2 m grid model. It can be seen that the span affects the deflection more significantly compared to the height of the model. The maximum nodal deflection was also checked against the limiting deflection value (span/360). All models were found to satisfy the deflection check, in which the maximum deflections are less than the limiting value of 5 mm and 11 mm for 2×2 m and 4×4 m grid models, respectively.

TABLE 4. Comparison of maximum nodal displacement for different span

Height (m)	2×2 m grid model	4×4 m grid model	Deflection check
0.5	-0.0216	-0.0929	PASS
1.0	-0.0134	-0.0567	PASS
1.5	-0.0132	-0.0548	PASS

Note: The negative sign denotes downward deflection.

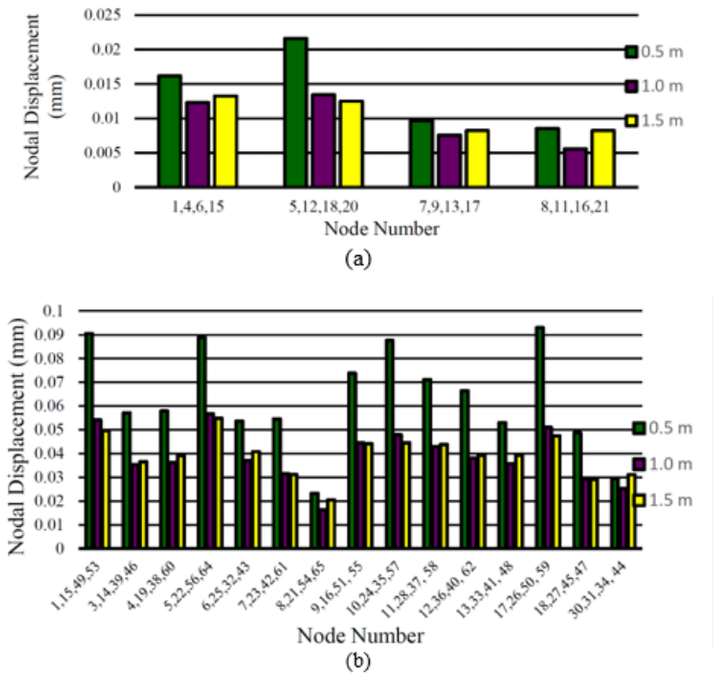

FIGURE 4. Nodal displacements for (a) 2 × 2 m grid model and (b) 4 × 4 m grid model

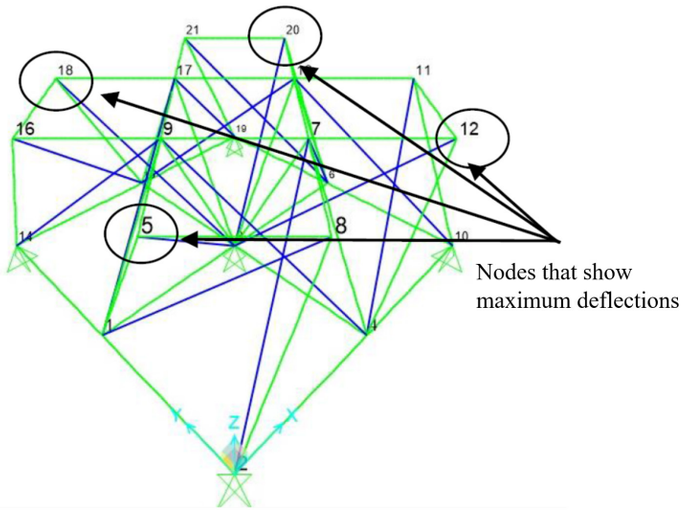

FIGURE 5. Nodes with maximum nodal displacements for 2 × 2 m grid model

DEFLECTED SHAPE OF THE MODELS

Figure 6 presents the deflection profile for 2×2 m and 4×4 m grid model. Grey colour denotes the deflected shape model, whereas blue and green colours indicate the struts and the cables at original positions, respectively. It shows that the model bends in sagging, which the sagging is more obvious in the 4×4 m grid model than in the 2×2 m grid model due to the longer span.

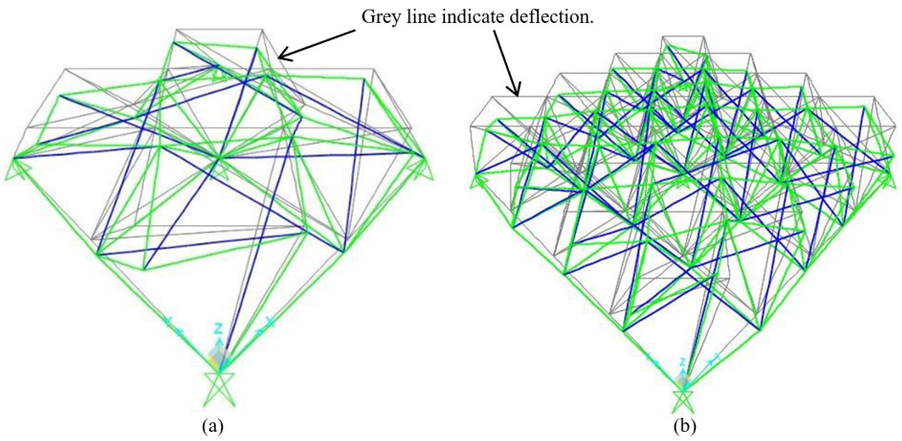

FIGURE 6. Deflection shape for (a) 2 × 2 m grid model and (b) 4 × 4 m grid model

AXIAL FORCES

The load combination case ULS 2 resulted in the most critical value of axial forces in all the tensegrity models; therefore, the axial forces are presented in the section. Since the analysis results are comprehensive for the 4×4 m grid model and due to symmetry in geometry, only a quarter of the model is presented. Figure 7 and Figure 8 illustrate the axial forces for struts and cables of different heights for the 2×2 m and 4×4 m grid model. There is no specific trend regarding axial forces on the struts and cables due to the various heights of the model.

The axial forces must be checked against the upper and lower axial force limits as shown in Equation 3, to ensure the model performs in an elastic range. It is found that the axial forces for struts are within the permissible limits. However, there are several cable members that are slackened due to the cables in negative forces (compression). The slackened cables occurred due to insufficient pre-stressing forces Liew et al. (2001). If the cables are not pre-stressed, slackening can occur in the cables when multiple loads are applied. However, from the design report, due to inherent redundancy, the cables that are slackened pose no damage towards the model.

STRUTS' DEMAND CAPACITY RATIO (DCR) FOR DIFFERENT DIAMETER

In the first phase, tensegrity grid models with struts of an outer diameter of 76.1 mm demonstrate nodal displacements within the permissible limit. This section presents an assessment on the demand capacity ratio (DCR) based on a comparative analysis of grid models featuring different strut diameters, aiming to determine an optimised section. Figures 9 (a), (b), and (c) depict the demand capacity of these models across various strut diameters (21.3 mm, 48.3 mm, and 76.1 mm), with the DCR represented on a color scale ranging from 0 to greater than 1.0. In the color scale, red denotes a DCR exceeding 1.0, indicating that the member has surpassed its ultimate carrying capacity. Cyan represents a DCR below 0.5, signifying that the member achieves less than half of its ultimate carrying capacity. Other colors correspond to DCR values ranging from 0.5 to 1.0.

Figure 10 (a) further illustrates the demand-capacity ratio of these models across different strut diameters. Notably, the DCRs for all 76 mm diameter struts are approximately 0.0, suggesting a significant underutilization of the strut size and its carrying capacity to sustain loads. Conversely, DCRs for all 21.3 mm struts exceed 1.0, indicating the failure of these struts to support the applied loads adequately. Among the three diameters, the 48.3 mm struts achieve a DCR of 70-80%, representing the most efficient size. The DCR increases as the strut diameter decreases, aligning well with the findings of a prior study by Ruth et al. (2006).

Figure 10 (b) presents the empirical equations that correlate DCR with strut diameter. On the basis of the equations DCR can be correlated to strut diameters with logarithmic regression at high correlation coefficient R^2 value (more than 0.94). Two equations from a set of data are conventionally used; representing the upper and lower bounds. The results led to a linear trend of gradually decrease of DCR over the strut diameter. This developed linear regression model in this study can be used to identify the optimised strut diameters in tensegrity roof presented in the study, at desired DCR but less than 1.

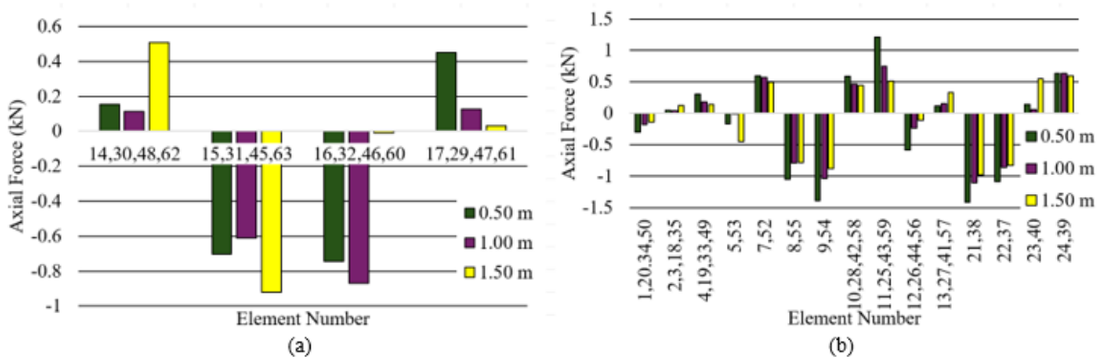

FIGURE 7. Axial forces for 2×2 m grid model : (a) struts and (b) cables

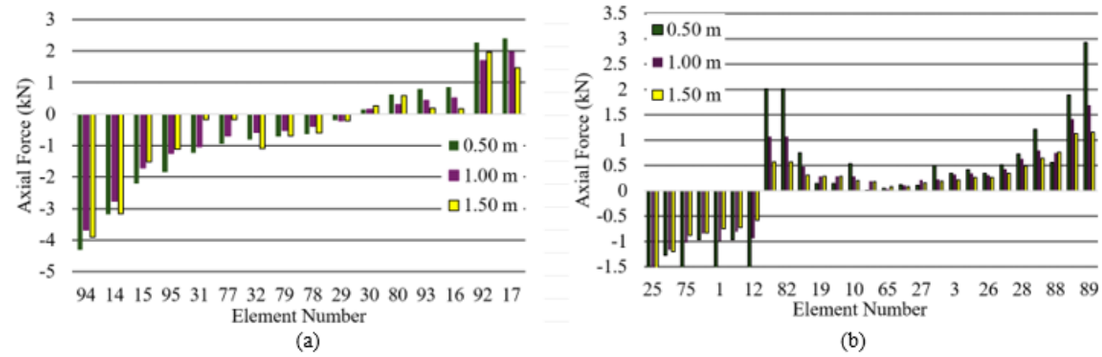

FIGURE 8. Axial forces for 4×4 m grid model: (a) struts and (b) cables

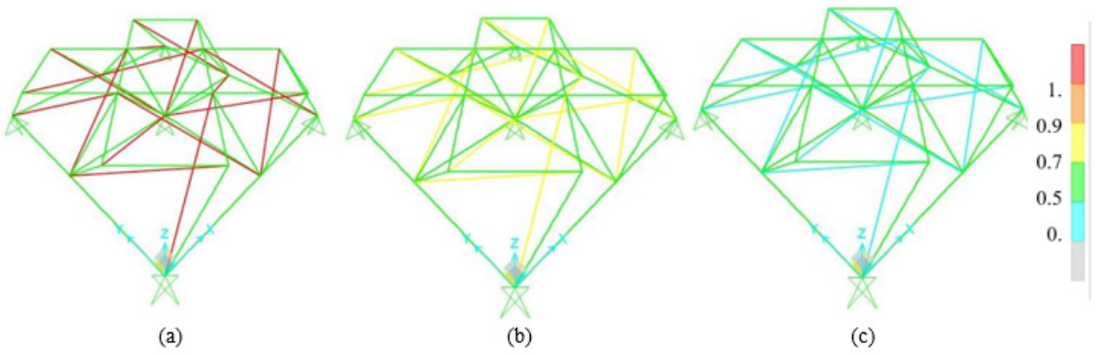

FIGURE 9. Demand capacity ratio in struts for (a) diameter 21.3 mm, (b) diameter 48.3 mm, and (c) diameter 76.1 mm

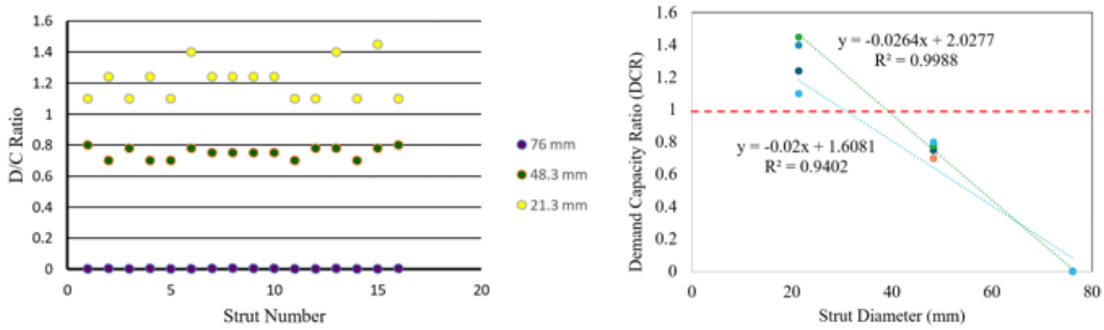

FIGURE 10. Demand capacity ratio of struts with different diameters

CONCLUSION

The study analyses and design the half-cuboctahedron tensegrity roof grid models using SAP2000. Several conclusions can be drawn from the study as follows:

1. Greater height of tensegrity roof grid model offers better deflection control. However, the increased height has minimal impact on the deflection when the section adequately carries the loads. Specifically, no significant effects on deflections were recorded between heights of 1.0 m and 1.5 m in this study.
2. Greater span of tensegrity roof grid model resulted in higher deflection. 4×4m grid model exhibits a higher deflection compared to 2×2m grid model. Higher deflections were recorded at nodes subjected to loadings and far away from the supports.
3. No clear trend can be discerned regarding the axial forces in struts and cables with varying heights. Due to inherent redundancy, the slackened cables pose no damage towards the model.
4. The demand-capacity ratio increases when the diameter of the strut decreases. It is found that the struts with diameter 48.3 mm are the optimum size to be used for the tensegrity roof model.

Understanding the relationship between geometry, section properties, and the behaviour of tensegrity roofs is crucial for guiding innovative design and optimising fabrication processes. Current research primarily focuses on the theoretical aspects of tensegrity structures, such as their fundamental mechanics and performance analysis. Ongoing research and development are addressing these limitations, addressing more practical research on design, construction methods, and real-world applications, especially for large-scale projects. As new materials, fabrication techniques, and design tools emerge, the potential applications of tensegrity structures are likely to expand. Future studies should explore different forms of tensegrity beyond the cuboctahedron, varying spans and support locations, diverse pre-stressing forces, and curved or long-span roofs. Additionally, dynamic analysis, adaptive tensegrity roofs, and energy-efficient strategies should also be considered in future work.

APPENDIX

TABLE A1. Nodal coordinates

Node	Height 0.5 m, 1.0 m, 1.5 m		Height 0.5 m	Height 1.0m	Height 1.5 m	Location
	X	Y	Z	Z	Z	
1	0	1.0	0	0	0	Bottom
2	0	0	0	0	0	Bottom
		3 1.0 1.0 0		0	0	Bottom
4	1.0	0	0	0	0	Bottom

continue ...

... cont.

5	0	0.5	0.5	1.0	1.5	Top
7	1.0	0.5	0.5	1.0	1.5	Top
8	0.5	0	0.5	1.0	1.5	Top
9	0.5	1.0	0.5	1.0	1.5	Top

TABLE A2. Element connectivity of cables

Element	Node *i*	Node *j*	Element	Node *i*	Node *j*
1	1	2	10	9	5
2	1	3	11	9	7
3	4	3	12	8	7
4	4	2	13	8	5
5	1	5	14	2	7
7	4	7	15	4	9
8	8	2	16	8	5
9	9	3	17	9	8

ACKNOWLEDGEMENT

The authors would like to thank Universiti Teknologi MARA for the support.

DECLARATION OF COMPETING INTEREST

None.

REFERENCES

Branam, N. J., Arcaro, V. & Adeli, H. 2019. A unified approach for analysis of cable and tensegrity structures using memoryless quasi-newton minimization of total strain energy. *Engineering structures* 179: 332-340.

de Albuquerque, N. B., Gaspar, C. M., Seixas, M., Santana, M. V. & Cardoso, D. C. (2022). Design, fabrication and analysis of a bio-based tensegrity structure using non-destructive testing. *Engineering structures* 265: 114457.

Gómez-Jauregui, V., Carrillo-Rodríguez, Á., Manchado, C. & Lastra-González, P. 2023. Tensegrity applications to architecture, engineering and robotics: A Review. *Applied Sciences* 13(15): 8669.

Hanaor, A., & Liao, M.-K. 1991. Double-layer tensegrity grids: static load response. Part I: analytical study. *Journal of structural engineering* 117(6): 1660-1674.

He, J., Wang, Y., Li, X., Jiang, H. & Ye, Z. 2024. A modified dynamic relaxation form-finding method for general tensegrity structures with inextensible tensile members. *Computers & Structure*s 291: 107204.

Liew, J. R., Punniyakotty, N. & Shanmugam, N. 2001. Limit-state analysis and design of cable-tensioned structures. *International journal of space structures* 16(2): 95-110.

Martínez, Á. O. G., Rangel, J. M. H., y Hernandez, M. A. P. L., Contreras, M. A., Zaragoza, J. B. H., Rea, L. P., Lara, T. L. & Gonzalez, E. R. 2019. Dynamical Behavior of a Tensegrity Structure Coupled to a Spatial Steel Grid. *Current Journal of Applied Science and Technology* 38: 1-24.

Oh, C. L., Choong, K. K. & Low, C. Y. 2012. Biotensegrity inspired robot–Future construction alternative. *Procedia Engineering* 41: 1079-1084.

Oh, C. L., Choong, K. K., Nishimura, T. & Kim, J.-Y. 2020. Form-finding of spine inspired biotensegrity model. *Applied Sciences* 10(18): 6344.

Oh, C. L., Choong, K. K., Nishimura, T. & Kim, J.-Y. 2022. Multi-directional shape change analysis of biotensegrity model mimicking human spine curvature. *Applied Sciences* 12(5): 2377.

Panigrahi, R., Gupta, A. & Bhalla, S. 2009. Dismountable steel tensegrity grids as alternate roof structures. *Steel and Composite Structures* 9(3): 239-253.

Parthasarathi, N., Satyanarayanan, K., Prakash, M. & Sulaiman, S. 2016. Comparison of the performance of hexagonal grid and half-cuboctahedron grid tensegrity systems in roof structures. *Indian Journal of Science and Technology.*

Quirant, J., Kazi-Aoual, M. & Motro, R. 2003. Designing tensegrity systems: the case of a double layer grid. *Engineering structures* 25(9): 1121-1130.

Ruth, P., Marchand, K. A. & Williamson, E. B. 2006. Static equivalency in progressive collapse alternate path analysis: Reducing conservatism while retaining structural integrity. *Journal of Performance of Constructed Facilities* 20(4): 349-364.

Sulaiman, S., Parthasarathi, N., Geetha, B. & Satyanarayanan, K. 2016. The performance of half-cuboctahedron grid tensegrity systems in roof structures. *Indian Journal of Science and Technology*.